

Appendix - 2

Compilation of X-ray Diffractograms

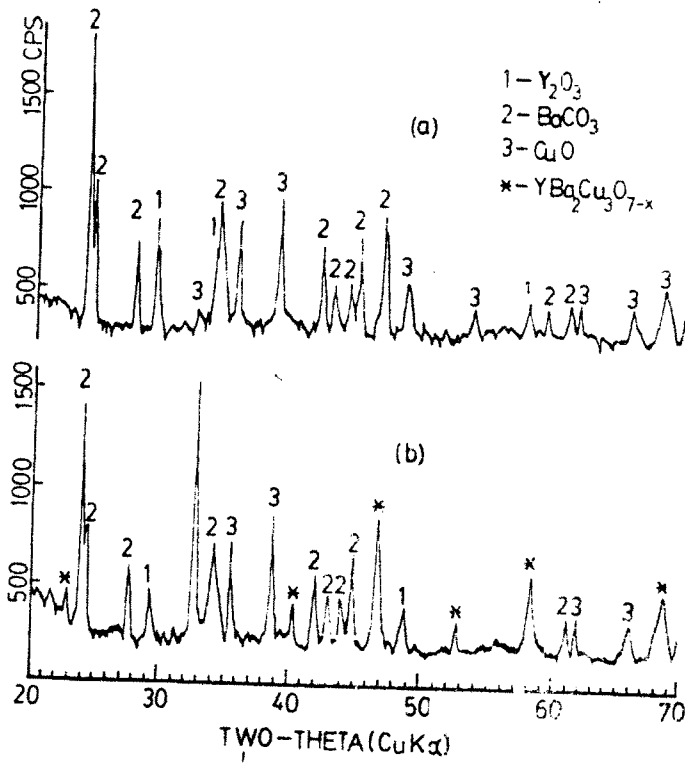


FIG. 1  
 The formation of tetragonal structure

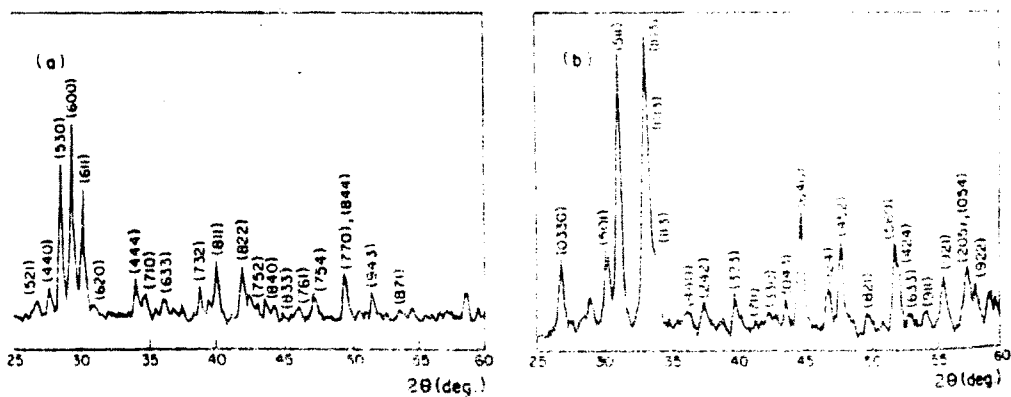


FIG. 2  
 X-ray diffraction pattern for (a)  $BaCuO_2$  and (b)  $Y_2Cu_2O_5$ .

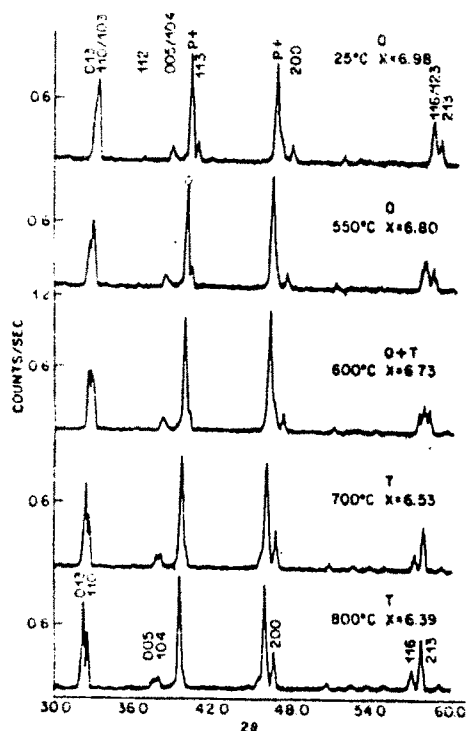


FIG. 3:

Powder x-ray data as a function of temperature in air. The Pt peaks are from the strip heater and were used as an internal calibration.

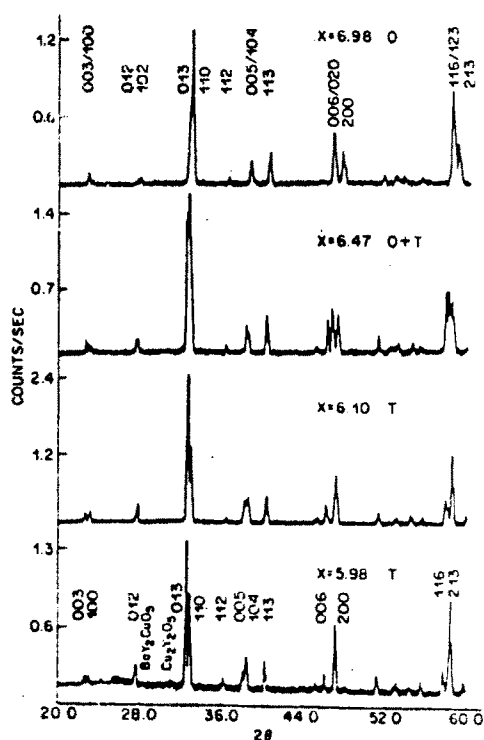


FIG. 4

Powder diffraction data for samples heated in  $N_2$  to adjust oxygen stoichiometry. The stoichiometry based on weight change is indicated on each panel.

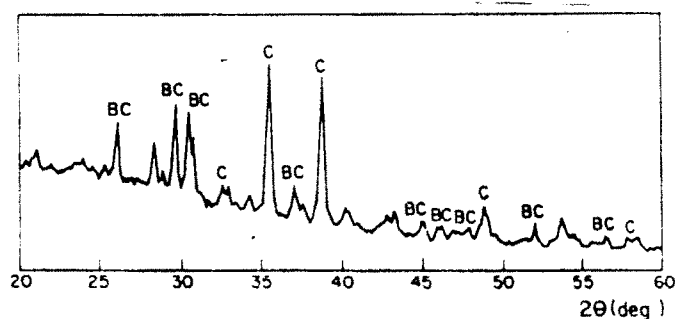


FIG. 5

X-ray diffraction patterns for molten phases bred out during the calcination of  $1/2Y_2O_3$ ,  $2BaCO_3$ , and  $3CuO$  at  $940^\circ C$  in air.

BC:  $BaCO_4$  ( $BaO_2 + CO_2$ , JCPDS CARDS #3-0659)

C:  $CuO$  (JCPDS CARDS #5-0661)

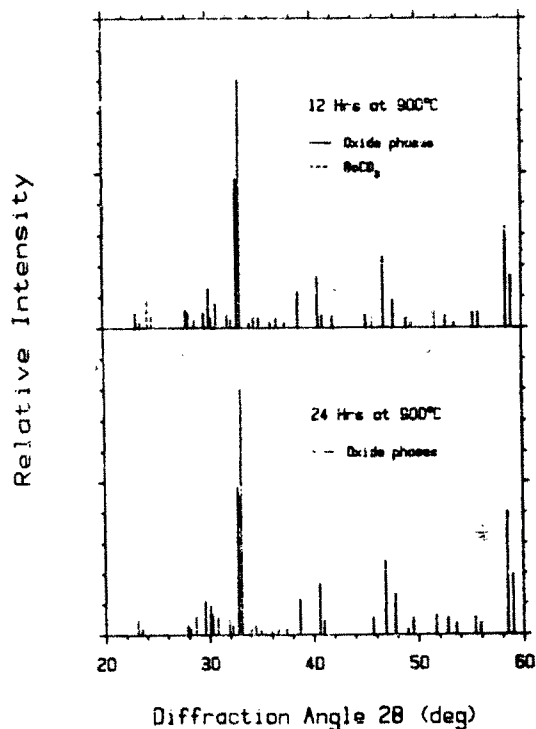


Fig. 6. X-ray diffraction patterns of a mixture of BaCO<sub>3</sub>, Y<sub>2</sub>O<sub>3</sub> and CuO heated at 900°C showing the presence of unreacted BaCO<sub>3</sub> after 12 hrs and a multiphase product after 24 hrs.

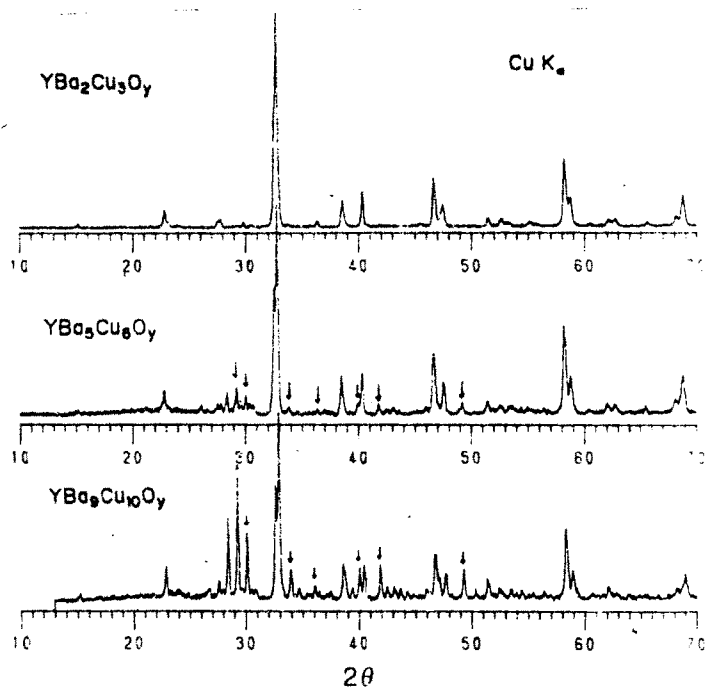


FIG. 7  
Powder X-Ray Diffractions. Diffractions due to BaCuO<sub>2</sub> are shown by arrows.

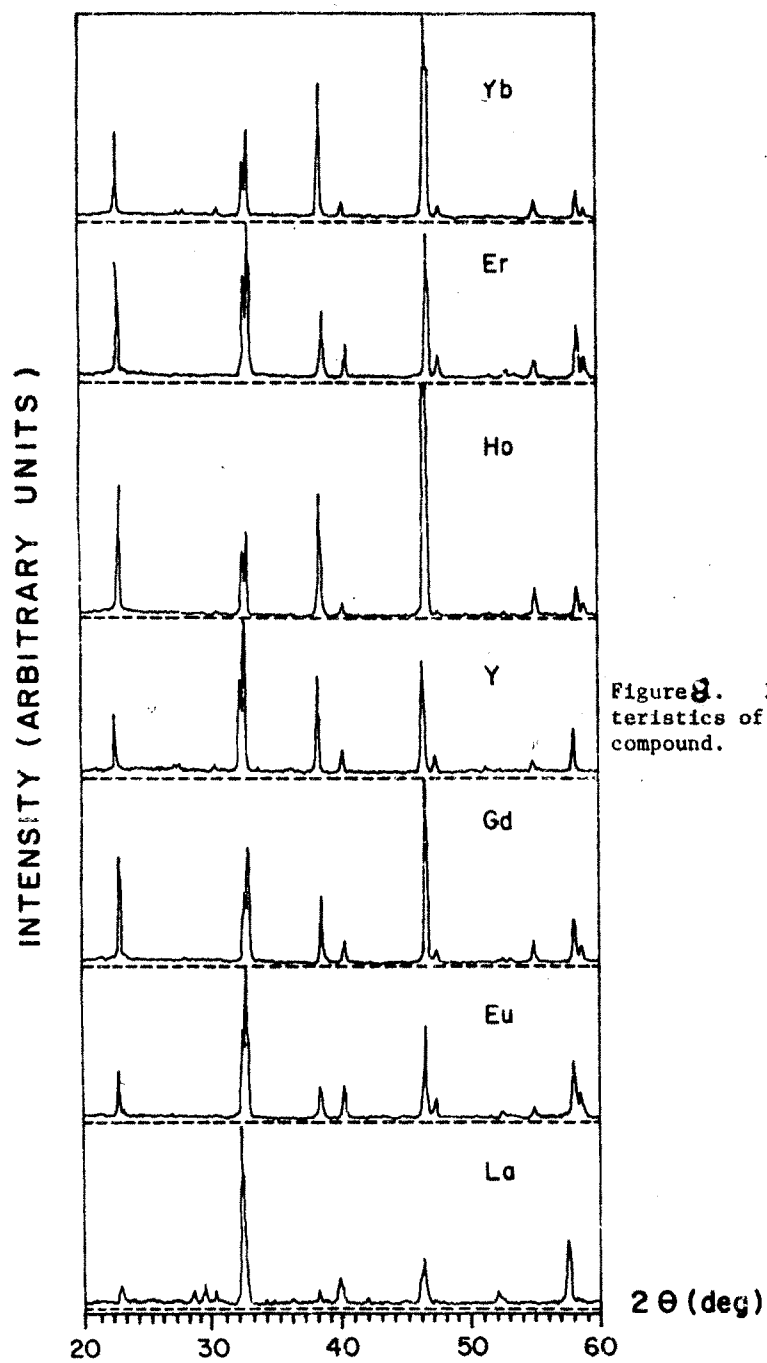


Figure 8. X-ray characteristics of some (1:2:3) compound.